Colloid Polym Sci 279:427–433 (2001)

ORIGINAL CONTRIBUTION

A. Tsuchida
H. Yoshimi
K. Ohiwa
T. Okubo

Rotational diffusion of tungstic acid colloids in microgravity studied by free-fall experiments. Effects of sodium chloride and ethyl alcohol

Received: 5 July 2000
Accepted: 21 September 2000

A. Tsuchida · H. Yoshimi · K. Ohiwa
T. Okubo (✉)
Department of Applied Chemistry
Faculty of Engineering, Gifu University
Yanagido 1-1, Gifu 501-1193, Japan
e-mail: okubotsu@apchem.gifu-u.ac.jp
Fax: +81-58-2932628

Abstract Rotational relaxation times (τ) of anisotropic tungstic acid colloids in aqueous suspension containing sodium chloride or ethyl alcohol are studied in microgravity achieved by free-fall experiments. Experimental errors at 0 *G*, in many cases, are small compared with those at 1 *G*, which is ascribed to the lack of the convection of suspension in microgravity. Much more reliable data of the diffusion coefficients are obtained in microgravity. The limiting slopes of the relaxation curves in the plots of the transmitted-light intensity against time at 1 *G* depend on the flow direction of the suspension in the flow cell, whereas those at 0 *G* are close to zero irrespective of the flow direction. Sodium chloride decreases τ, whereas ethanol addition increases this time. These effects are ascribed to the thinning of the electrical double layers and to the increase in the suspension viscosity.

Key words Rotational diffusion · Tungstic acid colloid · Microgravity effects · Free-fall experiments · Electrical double layers

Introduction

Recently, keen attention has been paid to microgravity experiments for the physicochemical properties of colloidal suspensions [1–11]. It should be noted that the gravitational effect is significant for the translational and rotational diffusion of colloidal particles larger than 0.1 μm and heavier than 0.1 in the density difference of the particles against solvent ($\Delta\rho$). The Péclet number, P_e, which is the ratio of the time of sedimentation of a sphere in gravity against that of translational Brownian diffusion, is one of the convenient parameters to know the gravitational effect compared with the Brownian diffusion [12–15].

$$P_e = rS/D_t = \left(4\pi r^4 \Delta\rho g\right)/(3k_B T) \ , \qquad (1)$$

where r is the sphere radius, S and D_t the sedimentation and translational diffusion coefficients, g the gravitational acceleration, k_B the Boltzmann constant and T the absolute temperature, respectively.

For tungstic acid colloids the Péclet number is estimated to be about 230 when a sphere of 1.5-μm radius and with a specific gravity of 5.5 is assumed in water suspension. The Péclet number shows that the contribution of the sedimentation is much larger than that of diffusion.

The sedimentation of nonspherical particles such as tungstic acid colloids is complicated by the fact that the translational and rotational motions are coupled. The particles sediment in a direction that depends on their orientation. Rotational Brownian motion changes the orientation of the particles and hence their sedimentation speeds and directions; however, on average, the particles will move in the direction of gravity only. For homogeneous particles the average sedimentation velocity equals that of spherical particles.

Flow birefringence, non-Newtonian flow, electric birefringence, fluorescence depolarization and dielectric dispersion are typical methods for the determination of the rotational diffusion coefficients (D_r) [16–20]. One of the authors has proposed a stopped-flow technique as a new and convenient method for determining the rotational relaxation time, τ (ranging from 1 ms to several seconds) of anisotropic colloidal particles such as

ellipsoidal colloids of tungstic acid [21]. The important role of the electrical double layers on the rotational diffusion has been clarified. Under gravity exact values of τ are difficult to measure owing to the convection of the suspension and the sedimentation of anisotropic colloids accompanied with the birefringence flow. For the study of the rotational relaxations monodispersed colloids of tungstic acid have many advantages, such as chemical stability, uniformity in their size, etc. The duration of the microgravity obtained by the present free-fall facility is short, 4.5 s. However, tungstic acid colloids are quite appropriate for the free-fall experiments, since their rotation is complete within about 4 s.

In a previous report [22], the rotational relaxation times of tungstic acid colloids in aqueous media were determined in microgravity. Much more reliable data of the diffusion coefficients were obtained in microgravity, and τ and D_r in microgravity were quite the same as those in gravity. Furthermore, the very important role of the electrical double layers formed around the particles for the rotational diffusion has been clarified both in microgravity and in gravity. The accurate thickness of the layers has been evaluated in microgravity.

In this work, the D_r values in microgravity were studied in the presence of sodium chloride and ethyl alcohol.

Experimental

Materials

Tungstic acid was prepared and purified by the method of Furusawa and Hachisu [23]. 1 N HCl (25 ml, Wako Pure Chemical Industries, Osaka) and 7 wt% Na_2WO_4 (50 ml, purity greater than 99%, Wako) were kept at 0–5 °C separately for more than 10 h before mixing. Then the two solutions were mixed homogeneously at once, and the mixture was left at room temperature for more than 10 h. A slightly yellowish gel of tungstic acid colloids was obtained. The gel was poured into 200 ml water, and then the suspension was stirred thoroughly. The suspension thus obtained was centrifuged (Kokusan, type H-9R, Tokyo) at 5000–6000 rpm for 480 s. The dispersion and the centrifuge processes were repeated five times, and the suspension (1.2 l) was incubated in a thermostated bath (changed from −1 to 30 °C) for more than 12 h. Then the monodispersed crystalloids appeared. The colloids thus obtained were further purified by repeated decantation.

The major ($2c$) and middle ($2b$) axes of the colloids obtained (W1-W44) were determined using a metallurgical microscope (Olympus, PME3, Tokyo, ×400–1000). The cell used for the microscope observation was the same as that described in a previous report [21]. The size of the particles increased as the incubation temperature increased as is shown in Fig. 1. The colloids were also obtained by incubation in an aqueous ethylene glycol mixture, where small colloids were obtained compared with those prepared in water at the same temperatures. The minor axis ($2a$) was not determined experimentally in this work but was estimated from the data of previous work [23] on electrophoresis measurements. The $2a$ values were estimated to be between 0.01 and 0.09 μm [24–26]. The $2c$, $2b$ and $2a$ values of the W41 sample used in this work were 2.95, 1.34 and 0.075 μm, respectively. It should be noted that τ is very insensitive to the $2a$ value itself.

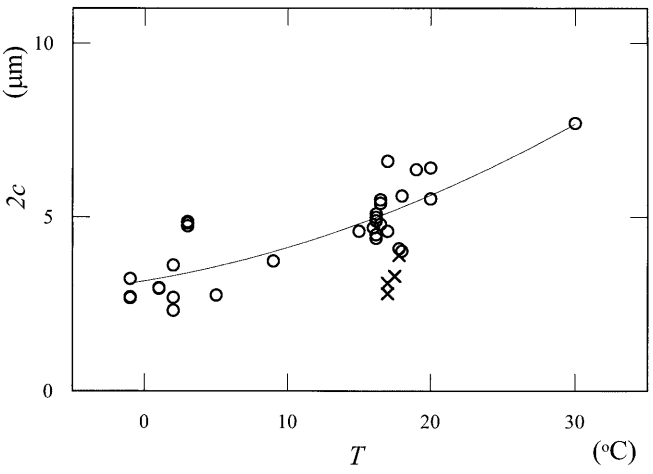

Fig. 1 Temperature dependence of the major axis length of the tungstic acid colloids formed. ○: in water, ×: in water–ethylene glycol mixtures

The relationship between $2b$ and $2c$ for the samples prepared in this work is shown in Fig. 2. The theoretical τ values were calculated from Perrin's equation [27] using the observed $2c$ and $2b$ values. As for the relationship between the values of b and c, $b = 0.41c$ was observed in our previous publication [22]. Note that Suda and Imai [28] reported a relation of $b = 0.30c$ for the same colloids, though their photographs showed a thin rectangle instead of an ellipsoid. Furusawa and Hachisu [24, 25] have reported the transformation of shape from ellipsoidal to rectangular with time.

The water used for the preparation of the sample suspensions was obtained from a Milli-Q water system (Millipore, Milli-RO Plus and Milli-Q Plus, Bedford, Mass.). Ethylene glycol and ethanol were the purest grades available commercially (Wako Chemicals, Osaka). Volumetric analysis grade sodium chloride solution (1 mol/l) was purchased from Wako Chemicals. The deionization of the suspension was not made in this work with coexistence of mixed beds of cation- and anion-exchange resins, since the resins exchange all the colloidal particles (slightly water soluble) with hydroxide ions from the dissociation of water.

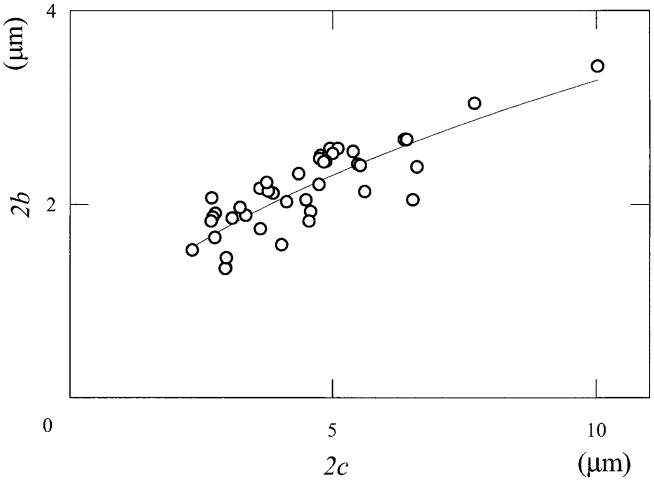

Fig. 2 Relationship between the major axis ($2c$) and the middle axis ($2b$) of tungstic acid colloids (W1-W44)

Measurements of rotational relaxation time

The rotational relaxation times (τ) were measured from the traces of the transmitted-light intensity with time just after stopping the flow using a device as shown in Fig. 3. The instrument consists of a quartz flow cell (inner size: $1 \times 5 \times 40$ mm, Nakamura Glass Co., Kyoto), solenoid valves, Phamed tubes (inner diameter: 3.1 mm) and a peristaltic pump (Masterflex, 7524-10, Ill.). The pump circulates the colloidal suspension (about 40 ml) at a flow rate of 30 ml/min. Light from a light emitting diode (LED, Sansui, 12 V, 600–800 nm) passes through the cell and the transmitted-light intensity is measured on a photodiode (Hamamatsu Photonics, S2281-01, Hamamatsu). A half mirror and another photodiode to compensate fluctuation of the light intensity from the LED were not used in this experiment because the stability of the intensity in microgravity has already been proven [22]. The signal from the photodiode was led into a preamplifier (Hamamatsu, C2719) and into a homemade offset main amplifier. The total rise time of the instrument was less than 7 μs. The signals were finally recorded on an analogue-to-digital (A/D) converter [Contec, AD12-8(PM), Osaka, 10 μs interval] built in a personal computer (NEC, PC9821, Tokyo) and further on a backup A/D converter of the free-fall facility. The signal was recorded from 2 s before dropping to 12 s after stopping the free-fall capsule. All the optical components are fixed tightly in a firm aluminum measurement box. The flow directions of the sample suspension in the observation cell are shown in Fig. 3. For the four flow directions (abbreviated as up, down, back and side) τ values were measured at 1 G and 0 G. The emitted light always hits the cell perpendicular to the largest plane.

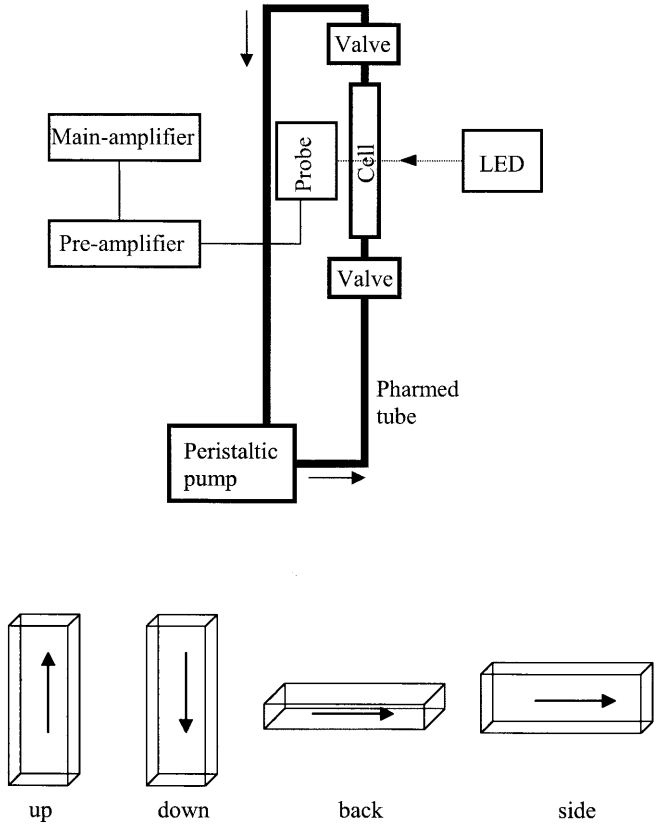

Fig. 3 Block diagram of the instrument (*upper*) and the flow directions in the cell (*lower*)

The major axes of tungstic acid are oriented parallel to the flow direction in the cell during the continuous flow, which is due to the shearing forces arising from the velocity gradient. When the suspension flow is stopped, the colloidal particles revert to rotating freely in a Brownian random distribution. Translational diffusion is safely neglected in the stopped-flow method, since the flow of the solvent molecules stops completely when the observation starts. For our anisotropic-shaped colloids, the multiple scattering changes significantly with the orientation. Thus, the intensity of the transmitted-light decreases, relaxing toward an equilibrium point after the flow is stopped.

The rotational diffusion constant, D_r, is evaluated from the τ values using Eq. (2).

$$D_r = 1/6\tau \ . \tag{2}$$

The theoretical values of D_r of ellipsoids are obtained using Perrin's equation, Eq. (3) [27].

$$D_r = 3k_B T\left(a^2P + b^2Q\right)/16\pi\eta\left(a^2 + b^2\right) \ , \tag{3}$$

where k_B, T and η in Eq. (3) are the Boltzmann constant, the absolute temperature and the viscosity of the solvent, respectively. The constants P, Q and R are derived from Eqs. (4), (5) and (6).

$$P = \int_0^\infty \mathrm{d}s/\left(a^2 + s\right)\sqrt{(a^2 + s)(b^2 + s)(c^2 + s)} \ , \tag{4}$$

$$a^2P + b^2Q + c^2R = \int_0^\infty \mathrm{d}s/\sqrt{(a^2 + s)(b^2 + s)(c^2 + s)} \ , \tag{5}$$

$$P + Q + R = 2/abc, \quad a < b < c \ . \tag{6}$$

The microgravity experiments were performed at the free-fall facility of the Micro-Gravity Laboratory of Japan (MGLAB) in Toki, Gifu prefecture. The duration of the microgravity was about 4.5 s. The G values during the free-fall were ± 0.0003 for both horizontal and vertical directions. The changes in temperature, humidity and pressure inside the capsule at 0 G were small, ± 0.1 °C, $\pm 0.2\%$ relative humidity and ± 0.0015 kg/cm^2, respectively.

Results and discussion

Rotational relaxation in microgravity

A typical trace of the transmitted-light intensity is shown in Fig. 4. The measurements were made in pure water for the upward flow directions in microgravity. The ordinate designates the output voltage from a main amplifier. A high output means a high transmitted-light intensity, and the values in the figures include the offset from the absolute output. $t = 0$ is the time when the G sensor of the free-fall facility detected G values smaller than 0.1 and here the pump was stopped. Circulation of the suspension was stopped completely within 0.1 s after stopping the pump, which was confirmed by video camera observation. The high optical intensity and its pulse by the pump are observed at $t < 0$ s in the figure. After stopping the pump the output decreased. Around $t = 3$ s, the output converged to the limiting value, which indicates that an almost random orientation of the colloidal particles is attained. The straight solid line in the figure shows the least-squares linear fitting between

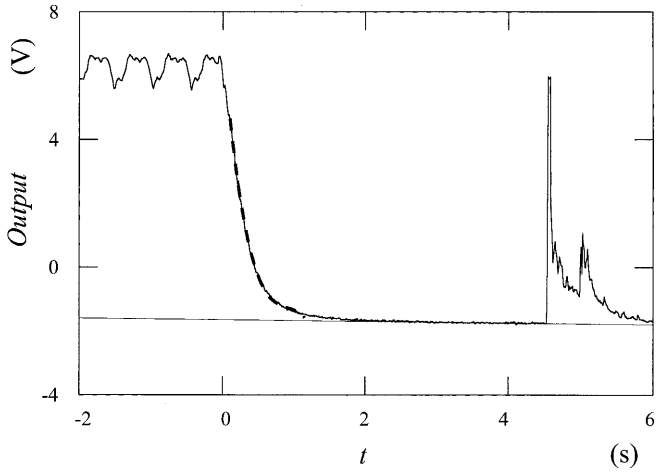

Fig. 4 An example of the rotational relaxation curves for W41 particles at 27.7 °C. 0 *G*, 0.20 wt%, "up" flow. *Solid line*: equilibrium linear fitting, *broken curve*: exponential fitting

$t = 4$ and 4.5 s. After subtracting the values of the linear fitting line from those of the original curve, the values were fitted by an exponential function and a vertical shift. The broken line shows the least-squares fitting and τ is obtained. The strange signal recorded at $t = 4.5$ s was caused when the capsule was stopped.

The slopes and τ values for the "up" and "side" flow directions are compared in Fig. 5 at 0 and 1 *G*. The slopes at 0 *G* were close to zero, whereas those at 1 *G* shifted to smaller and larger values for "up" and "side" flow directions, respectively. The average slopes were negative for "up", "down" and "back" directions, whereas that for the "side" direction was positive. On the other hand, the slope values at 0 *G* were always close to zero irrespective of the flow direction. These results were clearly explained by the sedimentation of the colloidal particle in the slender rectangular flow cell. The slopes obtained at 1 *G* scattered greatly when they were compared with those at 0 *G*. Though the τ values at 0 *G* were not different from those at 1 *G*, the experimental errors in τ decreased greatly at 0 *G* compared with those at 1 *G*. Lack of sedimentation and convection will be the main cause for these observations.

It should be noted here that the τ values observed were always larger than the calculated values from observed c and b using Eqs. (2), (3), (4), (5) and (6) as shown by the broken curve in the figure. This difference demonstrates the important role of the electrical double layers formed around the colloidal particles, as was discussed in a previous article [22].

The effective sizes including the thickness of the double layers for the minor, middle and major axes are given by $2a + 2D_l$, $2b + 2D_l$ and $2c + 2D_l$, respectively. Here, the thickness of the electrical double layer (D_l) is given by

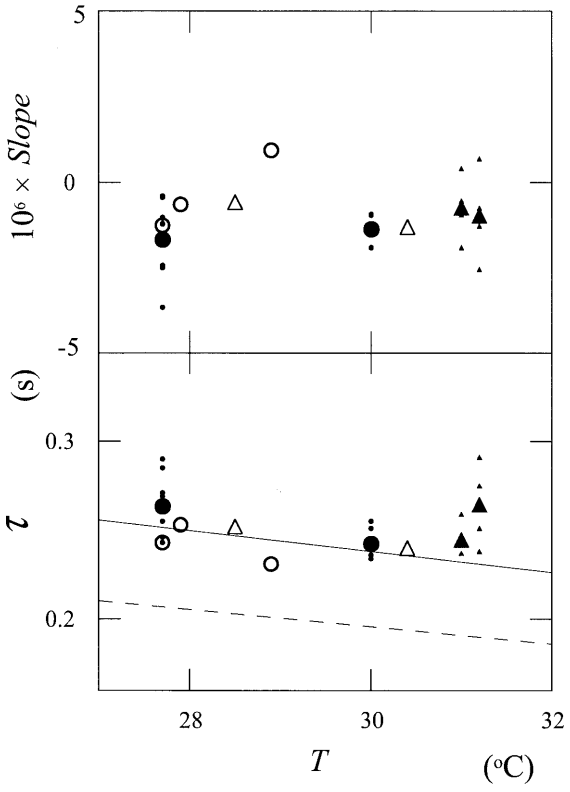

Fig. 5 Temperature dependence of the slopes and the rotational relaxation times (τ) of W41 particles. 0.20 wt%, ○: 0 *G*, "up", △: 0 *G*, "side", ●: 1 *G*, "up" and ▲: 1 *G*, "side". *Large marks* indicate the mean values. *Curves*: calculation from Perrin's equation, $D_l = 0$ nm (*broken*), $D_l = 50$ nm (*solid*)

$$D_l = (4\pi Bn)^{-1/2}, \tag{7}$$

where B is the Bjerrum length ($e^2/\varepsilon\, k_B T$, 7.19 Å at 25 °C) and n is the concentration of "free" (not bound to macroions) cations and anions in suspension. e and ε are the electronic charge and the dielectric constant of the solvent, respectively. In the absence of foreign salt, n corresponds to the "free" counterions (hydronium ions). The solid curve in the figure, which was almost fitted to the observed τ values at 0 *G*, was calculated when $D_l = 50$ nm was adopted. The importance of the "electrostatic" intermacroion repulsion by the electrical double layers has been pointed out for the physicochemical properties of various colloidal suspensions especially in salt-free systems [29–32]. The double layers were so soft that they were deformed and were even stripped away quite easily by the weak shearing forces.

The slopes and τ values are shown in Fig. 6 as a function of particle concentration. The former decreased slightly at low concentrations and then increased as the particle concentration increased. The latter decreased as the concentration increased, which is attributed to the thinning of the electrical double layers owing to the

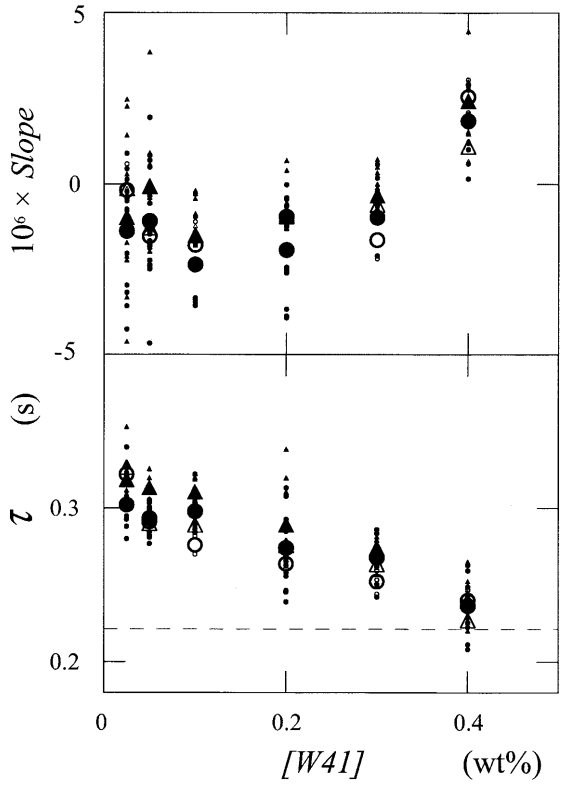

Fig. 6 Concentration dependence of the slopes and the rotational relaxation times (τ) of W41 particles at 25 °C. ○: 0 *G*, "up", △: 0 *G*, "side", ●: 1 *G*, "up" and ▲: 1 *G*, "side". *Large marks* are the mean values. *Broken line*: calculation from Perrin's equation ($D_l = 0$ nm)

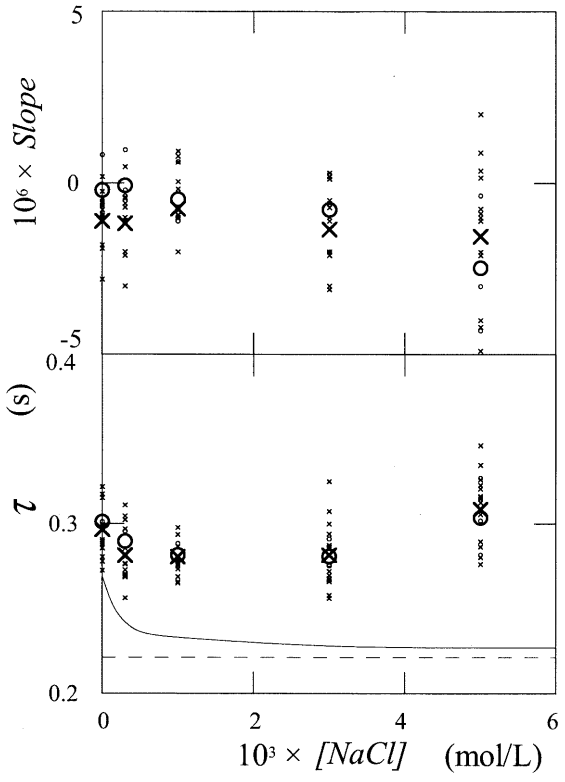

Fig. 7 Concentration dependence of the slopes and the rotational relaxation times (τ) of W43 particles at 25 °C. 0.20 wt %, "up" flow, ○: 0 *G*, ×: 1 *G*. *Large marks* are the mean values. *Solid curve*: calculation from Perrin's equation, *broken line*: calculation at $D_l = 0$ nm

increase in the ionic concentration of the suspension. Tungstic acid particles are very slightly dissociative in water. The broken curve indicates the calculation of the τ value from Eqs. (2), (3), (4), (5) and (6) and $D_l = 0$ nm. The difference between the observation and the calculation supports the important role of the electrical double layers. D_l values of 80 and 50 nm were estimated at 0 wt% (extrapolation) and 0.2 wt% of W41 particles, respectively, from Eqs. (2), (3), (4), (5) and (6). Equation (7) gives n values of 2.9×10^{-5} mol/l at 0 wt% and 7.4×10^{-5} mol/l at 0.2 wt%. Therefore, 4.5×10^{-5} mol/l tungstic acid is estimated to dissociate in water owing to the increase in concentration. It should be mentioned here that the experimental errors in τ decreased greatly at 0 *G* compared with those at 1 *G*.

Influence of sodium chloride

The concentration dependence of sodium chloride upon the slopes and τ values for the "up" direction is shown in Fig. 7. The slopes at 0 *G* with low concentrations of sodium chlorides were close to zero, whereas those at 1 *G* were negative owing to the sedimentation effect. Here, the slopes at an NaCl concentration of 0.005 mol/l were rather scattered, which is attributed to the occurrence of the slight aggregation of the particles at high ionic concentration as discussed later. τ decreased as the salt concentration increased in the range from 0 to 0.001 mol/l, which is explained safely by the thinning of the electrical double layers with the salt. The solid curve in the figure shows the calculated τ values from Eq. (7) and Eqs. (2), (3), (4), (5) and (6). The broken line in the figure indicates the calculated τ value using the real size of the colloids, i.e., $D_l = 0$ mm. In spite of the monotonous decrease in the calculated τ values for sodium chloride concentrations higher than 0.003 mol/l, the observed τ values began to increase accompanied by large experimental errors. Our microscope observation revealed that a few colloidal particles aggregate slightly at high salt concentrations. It should be noted that more reliable values of the slope and τ were obtained in microgravity.

Influence of ethyl alcohol

The slopes and τ values at 0 and 1 *G* are shown in Fig. 8 as a function of fraction (x) of ethanol in ethanol–water

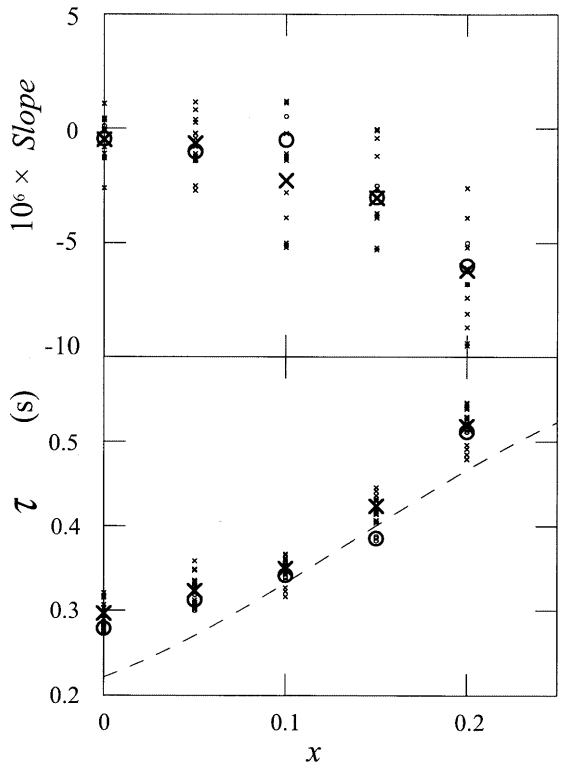

Fig. 8 Concentration dependence of the slopes and the rotational relaxation times (τ) of W43 particles at 25 °C. 0.20 wt%, "up" flow, ○: 0 *G*, ×: 1 *G*. *Large marks* are the mean values. *Broken line*: calculation from Perrin's equation ($D_l = 0$ nm)

mixtures for the "up" direction. The addition of ethanol should cause a change in the viscosity and the dielectric constant of the suspension. The τ values of the particles are dependent on T/η from Eq. (3) and on ε from Eq. (7). The slopes decreased as x increased. This is explained by the increase in suspension viscosity. The addition of ethanol increases the suspension viscosity, which results in larger τ values of the particles. The negative slopes at large x values are explained by the fact that the rotational relaxation was not complete within 4.5 s of measurement time. Interestingly, no microgravity effect is observed for the slopes. The τ values observed were still larger than the ones calculated from Perrin's equation (broken line). However, the difference between the observation and the calculation decreased as x increased except for $x = 0.2$. This is mainly due to the thinning of the electrical double layers owing to the decrease in ε with the addition of ethanol. A sharp increase in τ at 20 vol% of ethanol may again indicate the occurrence of the slight aggregation of the particles. It should be noted here that the slopes and τ values at 0 *G* were clearly not scattered so much compared with those at 1 *G*. This again supports the importance of the lack of sedimentation of the particles and no convection in microgravity for getting reliable data.

Acknowledgements The Promoting Committee of the Microgravity Experiments of Gifu Prefecture and the Space Forum Project (supported by the National Space Development Agency of Japan) are highly appreciated for their financial support. The authors thank the MGLAB, Toki, Gifu, for technical and financial support for the free-fall experiments.

References

1. (1985, 1986) Microgravity polymers. NASA Conference Publication C-2392, Cleveland, Ohio
2. Schiffman RA (ed) (1988) Experimental methods for microgravity materials science research, vol 2. 2nd International Symposium. TMS CD-ROM Library. TMS, Warrendale, Pa
3. Schiffman RA (ed) (1992) Experimental methods for microgravity materials science research, vols 4–8, 4th–8th International Symposia. TMS CD-ROM Library, TMS, Warrendale, Pa
4. Vanderhoff JW, El-Aasser MS, Micale FJ, et al (1986) PMSE Proc Am Chem Soc Div Polym Mat Sci Eng 54:584
5. Briskman V, Kostarev K, Leontyev V, Levkovich M, Mashinsky A, Nechitailo G (1997) Proceedings of the 48th International Astronomy Congress, Turin, Italy. International Astronomy Federation, pp 1–11
6. Zhu J, Li M, Rogers R, Meyer W, Ottewill RH, STS-73 Space Shuttle Crew; Russel WB, Chaikin PM (1997) Nature 387:883
7. Ishikawa M, Nakamura H, Kamei S, Okubo T, Morita TS, Kawasaki K, Kono Y (1996) J Jpn Soc Microgravity Appl 13:149–157
8. Ishikawa M, Nakamura H, Okubo T, Morita TS, Osada M, Tamaoki H, Kawasaki K, Oshikawa N, Nakamura Y, Nakakura T, Yoda S (1998) J Jpn Soc Microgravity Appl 15 Suppl II:168–172
9. Okubo T, Tsuchida A, Okuda T, Fujitsuna K, Ishikawa M, Morita T, Tada T (1999) Colloids Surf 153:515–524
10. Okubo T, Tsuchida A, Takahashi S, Taguchi K, Ishikawa M, Colloid Polym Sci 278:202–210
11. Okubo T, Tsuchida A, Kobayashi K, Kuno A, Morita T, Fujishima M, Kohno Y (1999) Colloid Polym Sci 277:474–478
12. Hunter RJ (1981) Zeta potential in colloid science. Principles and applications. Academic, London, p 117
13. Russel WB, Saville DA, Schowalter WR (1989) Colloidal dispersion. Cambridge University Press, Cambridge, p 394
14. van de Ven TGM (1989) Colloidal hydrodynamics. Academic, London, p 78
15. Hiemenz PC, Rajagopalan R (1977) Principles of colloid and surface chemistry, 3rd edn. Dekker, New York, p 176
16. Cohn EJ, Edsall JT (1943) Proteins, amino acids and peptides. Reinhold, New York
17. Weber G (1953) Adv Protein Chem 8:416
18. Jerrard HG (1959) Chem Rev 59:345
19. Frey M, Wahl P, Benoit H (1964) J Chim Phys 61:1005
20. Wierenga AM, Philipse AP, Reitsma EM (1997) Langmuir 13:6947

21. Okubo T (1987) J Am Chem Soc 109:1913
22. Okubo T, Tsuchida A, Yoshimi H, Maeda H (1999) Colloid Polym Sci 277:601–606
23. Furusawa K, Hachisu S (1966) J Chem Soc Jpn 87:118
24. Furusawa K, Hachisu S (1963) Sci Light 12:1
25. Furusawa K, Hachisu S (1963) Sci Light 12:15
26. Zocher VH, Jacobson K (1929) Kolloidchem Beih 28:168
27. Perrin F (1934) J Phys Radium 5:497
28. Suda H, Imai N (1985) J Colloid Interface Sci 104:204
29. Hachisu S, Kobayashi Y, Kose A (1973) J Colloid Interface Sci 42:342
30. Pieranski P (1983) Contemp Phys 24:25
31. Okubo T (1988) Acc Chem Res 21:281
32. Okubo T (1993) Prog Polym Sci 18:481